Reduction of Substituted Benzenediazonium Salts by Solvated Electrons in Aqueous Neutral Solution Studied by Pulse Radiolysis

Kim Daasbjerg*,† and Knud Sehested‡,§

Department of Chemistry, University of Aarhus, Langelandsgade 140, DK-8000 Aarhus C, Denmark, and Risø National Laboratory, Roskilde, Denmark

Received: April 5, 2002; In Final Form: August 27, 2002

A pulse radiolysis study of six parasubstituted benzenediazonium salts, $X-C_6H_4N_2^+$ [X = $COOC_2H_5$, F, H, CH_3, OCH_3, and $N(CH_3)_2$], has been carried out in neutral aqueous solutions, where the principal reductant is the solvated electron. In the first step, the solvated electron reduces the diazonium salts to the corresponding diazenyl radicals, $X-C_6H_4N_2^{\bullet}$, in a diffusion-controlled process. On a short time scale, $X-C_6H_4N_2^{\bullet}$ is either involved in an equilibrium reaction with the parent diazonium salt ($K > 100\ M^{-1}$) in which a $(X-C_6H_4)_2N_4^{\bullet+}$ adduct is formed or decays to the aryl radical, $X-C_6H_4^{\bullet}$, through the expulsion of dinitrogen. Simulation of this kinetic scheme allows us to make a rough determination of the rate constants involved. The rate constants for the formation of the adducts are in the range $(0.7-1.9) \times 10^7\ M^{-1}\ s^{-1}$, whereas the fragmentation rate constants are in the range $(0.4-4.0) \times 10^5\ s^{-1}$. The aryl radicals subsequently attack the diazonium salts mainly at the terminal nitrogen atom with rate constants of $(0.13-5.9) \times 10^7\ M^{-1}\ s^{-1}$, thereby forming the radical cations of the corresponding azobenzenes, $(X-C_6H_4)_2N_2^{\bullet+}$, or eventually the corresponding OH adducts, $(X-C_6H_4)_2N_2OH^{\bullet}$, upon further reaction with water. These intermediates were identified in pulse radiolysis by generating the very same species through an alternative pathway involving oxidation of the parent azobenzenes. The reaction between the aryl radical and the salt exhibits a clear substituent effect in the sense that the reactivity increases as the electron-donating power of the substituent is enhanced. This is attributed to the stabilizing effect exerted by electron-donating groups on radical cations. Thus, the radical cations can be detected only for the methoxy and dimethylamino groups, whereas for the other substituents the transformation of $(X-C_6H_4)_2N_2^{\bullet+}$ to $(X-C_6H_4)_2N_2OH^{\bullet}$ takes place instantaneously.

Introduction

Arenediazonium salts, ArN_2^+, are versatile compounds that have found widespread use in organic synthesis. Many books, chapters, and reviews have been devoted to the description of the rich chemistry of diazonium compounds.[1−4] Replacement reactions such as the classical Sandmeyer reaction and coupling reactions affording azo compounds (i.e., dyes) are examples of well-established and important chemical processes. Whereas the diazo group is maintained in coupling reactions, replacement reactions are characterized by the loss of the group. The latter are also termed dediazoniation processes, and mechanistically they may involve both heterolytic and homolytic pathways, depending on the exact reaction conditions and in particular which reagents other than the diazonium salt are present. For instance, in the Sandmeyer reaction, the arenediazonium salt is converted to the corresponding aryl halide in a homolytic pathway, promoted by the presence of catalytic amounts of cuprous halide acting as an efficient reductant. In the most recent studies, the focus has been on the mechanistic aspects of heterolytic processes,[5−10] whereas less attention has been paid to the homolytic counterparts.[11−14]

The present work is devoted to the study of the fundamental aspects of the homolytic dediazoniation pathway depicted in Scheme 1.

SCHEME 1

$$ArN_2^+ \xrightarrow{\text{electron transfer}} ArN_2^{\bullet} \longrightarrow Ar^{\bullet} + N_2$$

In the first step, ArN_2^+ is reduced by a suitable electron-transfer agent to the diazenyl radical, $ArN_2^{\bullet}$, that subsequently gives up dinitrogen to form the aryl radical, $Ar^{\bullet}$. Since arenediazonium salts are easily reduced, having reduction potentials of ca. 0.5 V versus NHE measured in sulfolan,[15] many different species may act as reductants. Usually, metal cations such as Sn(II), Cr(II), Ti(III), V(II), Fe(II) and in particular Cu(I) are employed,[4,16−20] but in this study we use one of the simplest yet most powerful reductants, the solvated electron (oxidation potential = −2.86 V vs NHE),[21] generated by means of pulse radiolysis. Another advantage of this approach is that $Ar^{\bullet}$ is formed in a selective process with no interaction from the electron-transfer agent in the follow-up reactions, as the case would be for metal reductants. This should make it possible to investigate the kinetic features of reactions involving $Ar^{\bullet}$ and ArN_2^+. The focus in this paper thus clearly differs from that in previous pulse radiolysis studies of diazonium salts,[22,23] where the purpose has been either to study second-order radical−radical processes by employing high radiation doses[22] or to initiate chain processes involving alcohols and radicals derived thereof.[23] In a subsequent paper, we will present the results pertaining to the other strong reductant generated in pulse radiolysis, the hydrogen atom.[24]

We selected a series of parasubstituted benzenediazonium salts [$X-C_6H_4N_2^+BF_4^-$, X = $COOC_2H_5$, F, H, CH_3, OCH_3,

* To whom correspondence should be addressed. E-mail: kdaa@chem.au.dk.
† University of Aarhus.
‡ Risø National Laboratory.
§ Present address: Strandhøjen 5, 4000 Roskilde, Denmark.

10.1021/jp025900b CCC: $22.00
Published on Web 10/30/2002

and $N(CH_3)_2$] as substrates in order to elucidate the influence of the substituent on the reactivity pattern not only of the different diazonium salts but also of the aryl radicals produced along the reduction pathway. The reductant employed (i.e., the solvated electron, e_{aq}^-) was generated along with the hydroxyl radical, $HO^\bullet$, and the hydrogen atom, $H^\bullet$, by radiation of water using high-energy electrons (eq 1).[21]

$$H_2O \xrightarrow{\text{ionizing radiation}} e_{aq}^-,\ HO^\bullet,\ H^\bullet,\ H^+,\ H_2O_2,\ H_2 \qquad (1)$$

The radiation chemical yields of the three principal radicals are $G(e_{aq}^-) \approx G(HO^\bullet) \approx 2.8 \times 10^{-7}$ mol J^{-1} and $G(H^\bullet) \approx 0.6 \times 10^{-7}$ mol J^{-1}. The procedure for scavenging $HO^\bullet$ and $H^\bullet$ usually involves *tert*-butanol (eqs 2 and 3, $k_2 = 6.0 \times 10^8$ M^{-1} s^{-1}, $k_3 = 1.7 \times 10^5$ M^{-1} s^{-1}) or 2-propanol (eqs 4 and 5, $k_4 = 1.9 \times 10^9$ M^{-1} s^{-1}, $k_5 = 7.4 \times 10^7$ M^{-1} s^{-1}).[25]

$$HO^\bullet + (CH_3)_3COH \xrightarrow{k_2} {}^\bullet CH_2(CH_3)_2COH + H_2O \qquad (2)$$

$$H^\bullet + (CH_3)_3COH \xrightarrow{k_3} {}^\bullet CH_2(CH_3)_2COH + H_2 \qquad (3)$$

$$HO^\bullet + (CH_3)_2CHOH \xrightarrow{k_4} (CH_3)_2\dot{C}OH + H_2O \qquad (4)$$

$$H^\bullet + (CH_3)_2CHOH \xrightarrow{k_5} (CH_3)_2\dot{C}OH + H_2 \qquad (5)$$

However, since scavenging of $HO^\bullet$ and $H^\bullet$ in the present case would be accompanied by scavenging of the aryl radical, $X-C_6H_4^\bullet$ (eqs 6 and 7, $k_6 = 6.6 \times 10^5$ M^{-1} s^{-1} and $k_7 = 1.2 \times 10^7$ M^{-1} s^{-1}),[26] generated along the reduction pathway of the diazonium salt, we accepted in most situations the presence of $HO^\bullet$ and $H^\bullet$, and rather attempted to take their reactions into account by studying them separately.[24]

$$C_6H_5^\bullet + (CH_3)_3COH \xrightarrow{k_6} {}^\bullet CH_2(CH_3)_2COH + C_6H_6 \qquad (6)$$

$$C_6H_5^\bullet + (CH_3)_2CHOH \xrightarrow{k_7} (CH_3)_2\dot{C}OH + C_6H_6 \qquad (7)$$

Experimental Section

The diazonium salts were prepared according to the general procedure described in ref 27. They were recrystallized from acetonitrile and diethyl ether before use. The procedure for synthesizing (*E*)-4,4′-dimethoxyazobenzene[28] and (*E*)-4,4′-bis-(dimethylamino)azobenzene[29] is described in the references listed. All other chemicals—perchloric acid, 2-propanol, *tert*-butanol, fumaric acid, Ar, O_2, and N_2O—were of the highest commercially available purity. The solutions were prepared in 100-mL syringes using triply distilled water. The diazonium salts were dissolved in the aqueous solution at the very last moment before the pulse radiolysis experiment in order not to form the corresponding substituted phenols in hydrolysis reactions involving the diazo group. This was also the reason that the maximum concentration of the salts never exceeded 0.2 M. Hydrolysis of the ester group in $C_2H_5OOC-C_6H_4N_2^+$ to a carboxylic acid did not take place. The syringes were covered with tinfoil to avoid photolysis of the labile diazonium salts. The pulse radiolysis experiments were performed on Risø's HRC linear accelerator, which delivered 10-MeV electrons in a single pulse with a maximum intensity of 1 A. The dose, which was determined with the ferrocyanide dosimeter using $\epsilon_{420} = 1000$ M^{-1} cm^{-1} and $G = 6.0 \times 10^{-7}$ mol J^{-1}, was in most cases 0.8−40 Gy in 1-μs pulses. The cylindrical cell had a radius of 0.6 cm and a length of 2.55 cm. The light-path length was 2 × 2.55 cm = 5.1 cm. The optical detection system consisted of a 150-W Varian high-pressure xenon lamp with increased intensity in short pulses, a Perkin-Elmer double quartz prism monochromator, and a Hamamatsu R955 photomultiplier. The data were recorded on a 125-MHz LeCroy 9400 digital oscilloscope and were transferred to a PC for further treatment.[30] The program Gepasi 3.21 was employed in the simulations of the kinetic traces.[31] All measurements were carried out at 20 °C.

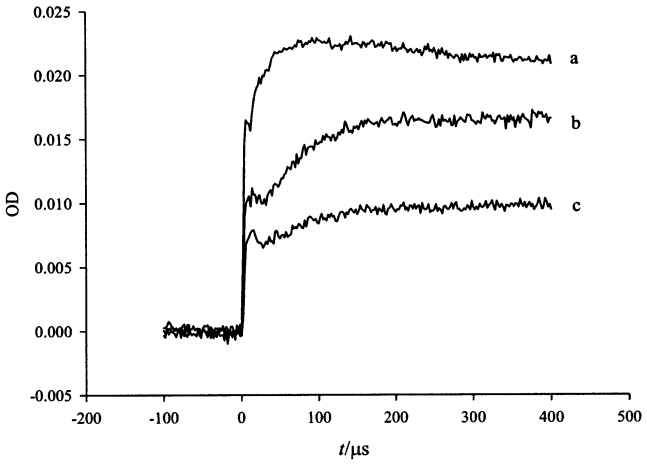

Figure 1. Traces of the transients recorded at 410 nm after a 2.5-Gy pulse on Ar-saturated neutral solutions of $C_6H_5N_2^+BF_4^-$: (a) 10^{-2} M, (b) 2.5×10^{-3} M, and (c) 6.25×10^{-4} M.

Results and Discussion

Figure 1 shows kinetic traces in terms of plots of the optical density (OD) versus time (*t*) obtained for three different concentrations of $C_6H_5N_2^+$ in an Ar-saturated neutral solution. In this solution, e_{aq}^- and $HO^\bullet$ are formed in equivalent amounts, accompanied by minor amounts of $H^\bullet$ (∼10%) upon radiolysis.

As seen, a buildup takes place within the first 100−400 μs, followed by a slow decay. The small spike observed at $t = 10$ μs is mainly due to the formation of the H adduct of the diazonium salt as described elsewhere.[24] Clearly, the buildup consists of two substrate-dependent parts that are assigned to the following sequence of reactions, eqs 8−13.

$$e_{aq}^- + X-C_6H_4N_2^+ \xrightarrow{k_8} X-C_6H_4N_2^\bullet \qquad (8)$$

$$X-C_6H_4N_2^\bullet + X-C_6H_4N_2^+ \underset{k_{-9}}{\overset{k_9}{\rightleftharpoons}} (X-C_6H_4)_2N_4^{\bullet+} \qquad (9)$$

$$X-C_6H_4N_2^\bullet \xrightarrow{k_{10}} X-C_6H_4^\bullet + N_2 \qquad (10)$$

$$X-C_6H_4^\bullet + X-C_6H_4N_2^+ \xrightarrow{k_{11}} (X-C_6H_4)_2N_2^{\bullet+} \qquad (11)$$

$$(X-C_6H_4)_2N_2^{\bullet+} + H_2O \underset{k_{-12}}{\overset{k_{12}}{\rightleftharpoons}} (X-C_6H_4)_2N_2OH^\bullet + H^+ \qquad (12)$$

$$\text{radicals} + \text{radical cations} \xrightarrow{k_{13}} \text{products} \qquad (13)$$

In the first step, eq 8, e_{aq}^- reduces the diazonium salt to the corresponding diazenyl radical, $X-C_6H_4N_2^\bullet$. This radical is either involved in an equilibrium reaction with the salt, eq 9, in which a $(X-C_6H_4)_2N_4^{\bullet+}$ intermediate is formed in the first substrate-dependent buildup or decays to the aryl radical, $X-C_6H_4^\bullet$, through the expulsion of dinitrogen, eq 10. The reactive aryl radical is the species that is then involved in the second substrate-dependent buildup, eq 11, where another radical

TABLE 1: Rate Constants (k) and Equilibrium Constants (K) for the Reactions of Parasubstituted Benzenediazonium Salts, Diazenyl Radicals, Aryl Radicals, and Radical Cations

X	k_8[a] 10^{10} M^{-1} s^{-1}	k_9[b] 10^7 M^{-1} s^{-1}	k_{-9}[c] 10^4 s^{-1}	K[d] M^{-1}	k_{10}[e] 10^5 s^{-1}	k_{10}[f] 10^5 s^{-1}	k_{10}[g] 10^5 s^{-1}	k_{11}[h] 10^6 M^{-1} s^{-1}	k_{11}[i] 10^6 M^{-1} s^{-1}	$k_{12/13}$[h] 10^3 s^{-1}
$COOC_2H_5$	5.5 ± 0.4	1.9 ± 0.6	2.7 ± 1.3	700 ± 410	0.8 ± 0.3	125		1.5 ± 0.5	2.5 ± 0.7	2.1 ± 1.0
F	6.0 ± 0.5	1.8 ± 0.5	7.3 ± 3.7	250 ± 140	4.0 ± 2.0			1.3 ± 0.4	1.3 ± 0.3	1.0 ± 0.5
H	5.8 ± 0.6	1.5 ± 0.5	9.3 ± 4.0	160 ± 90	2.0 ± 1.1	34	1.1	6.3 ± 2.0	6.4 ± 1.8	1.0 ± 0.4
CH_3	6.2 ± 0.4	0.7 ± 0.3	4.2[j]	170 ± 70	1.0[j]	23	1.6	9.0 ± 2.8	6.7 ± 2.4	3.0 ± 1.1
OCH_3	5.3 ± 0.4				1.0 ± 0.5[k]	15	1.7	28 ± 8[k]	20 ± 8	3.0 ± 0.9
$N(CH_3)_2$	5.6 ± 0.5	1.2 ± 0.4	7.0 ± 3.9	170 ± 110	0.4 ± 0.3	2	1.4	59 ± 20	49 ± 15	3.0 ± 0.7

[a] For the reaction of e_{aq}^- with the diazonium salts $X-C_6H_4N_2^+$. [b] For the buildup of $(X-C_6H_4)_2N_4^{\bullet+}$. [c] For the fragmentation of $(X-C_6H_4)_2N_4^{\bullet+}$. [d] $K = k_9/k_{-9}$ [e] For the fragmentation of $X-C_6H_4N_2^{\bullet}$; this study. [f] From ref 22 in *tert*-butanol/water. [g] From refs 35 and 36 in cyclopropane; values are extrapolated to 20 °C using the Arrhenius equation on the rate data listed at low temperatures. [h] Rate constant k_{11} for the buildup of $(X-C_6H_4)_2N_2^{\bullet+}$ and rate constant $k_{12/13}$ for the decay of $(X-C_6H_4)_2N_2^{\bullet+}$ or $(X-C_6H_4)_2N_2OH^{\bullet}$. Determined on the basis of simulation of the complete reaction scheme, eqs 9−13. [i] Determined from competition kinetics involving oxygen. [j] Selected as the upper limit; see text for discussion. [k] Determined on the assumption that there is no appreciable buildup of $(X-C_6H_4)_2N_4^{\bullet+}$ during the reaction; see text for discussion.

cation in terms of $(X-C_6H_4)_2N_2^{\bullet+}$ is formed. The $(X-C_6H_4)_2N_2^{\bullet+}$ species decays either through a reaction with water in which the corresponding OH adduct, $(X-C_6H_4)_2N_2OH^{\bullet}$, is generated, eq 12, or through different second-order reactions involving any of the radicals or radical cations present, eq 13. These reactions may also include reactive species originating from the processes of the other two principal radicals, $H^{\bullet}$ and $HO^{\bullet}$. In particular, for X = $COOC_2H_5$, F, H, and CH_3, the influence on the traces from the presence of OH adducts of the diazonium salts is nonnegligible, as discussed in our subsequent paper.[24] Below we describe the kinetic features of eqs 8−13 in detail.

Kinetics of Equation 8. The reaction between e_{aq}^- and $X-C_6H_4N_2^+$, eq 8, affording $X-C_6H_4N_2^{\bullet}$ is easily followed at the absorption maximum of e_{aq}^- at the wavelength $\lambda = 700$ nm. In Table 1, the rate constants measured for the different diazonium salts are collected. The fact that the rate constants are very large ($k_8 \approx 5.7 \times 10^{10}$ M^{-1} s^{-1}) and independent of the substituent is expected for a diffusion-controlled process involving two oppositely charged species. The data are in excellent agreement with similar pulse radiolysis data obtained in aqueous solution by Packer et al.,[23] whereas they are approximately a factor of 2 larger than those obtained in a *tert*-butanol/water mixture by Brede et al.[22]

Kinetics of Equations 9 and 10. The first substrate-dependent buildup we attribute to the formation of $(X-C_6H_4)_2N_4^{\bullet+}$ in the reaction between $X-C_6H_4N_2^{\bullet}$ and $X-C_6H_4N_2^+$, eq 9. The existence of such a species has, to the best of our knowledge, not been proposed previously. At low concentrations of the diazonium salt, the buildup of $(X-C_6H_4)_2N_4^{\bullet+}$ is hardly discernible in the kinetic traces for two reasons. First of all, the concentration of $(X-C_6H_4)_2N_4^{\bullet+}$ becomes small because of the presence of the reverse reaction of eq 9 and the relatively fast decay of $X-C_6H_4N_2^{\bullet}$ to $X-C_6H_4^{\bullet}$ in eq 10. Second, the trace is overlaid by signals from the strongly absorbing species formed in subsequent reactions, eqs 11 and 12. However, at high diazonium salt concentrations, or even better in the presence of 2-propanol, the kinetics of $(X-C_6H_4)_2N_4^{\bullet+}$ may be studied in detail.

One of the prominent features of 2-propanol is its effective scavenging of $HO^{\bullet}$, $H^{\bullet}$ (eqs 4 and 5), and $X-C_6H_4^{\bullet}$ (eq 7), thus leaving a simplified kinetic system consisting of eqs 9 and 10 as illustrated in Figure 2. Interestingly, $X-C_6H_4N_2^{\bullet}$ does not seem to abstract a hydrogen atom from 2-propanol with an appreciable rate as witnessed by the fact that almost the same OD of 0.04 is obtained in the presence and absence of 2-propanol at $t = 10$ μs; the optical density is slightly larger in the latter case because of contributions from the H and OH adducts of the salts. Furthermore, there is no decrease in OD upon adding additional 2-propanol. This result is somewhat surprising since it has been reported in the literature that a competition could be introduced between the first-order fragmentation reaction of the phenyldiazenyl radical and a second-order hydrogen atom abstraction from a compound such as toluene.[32]

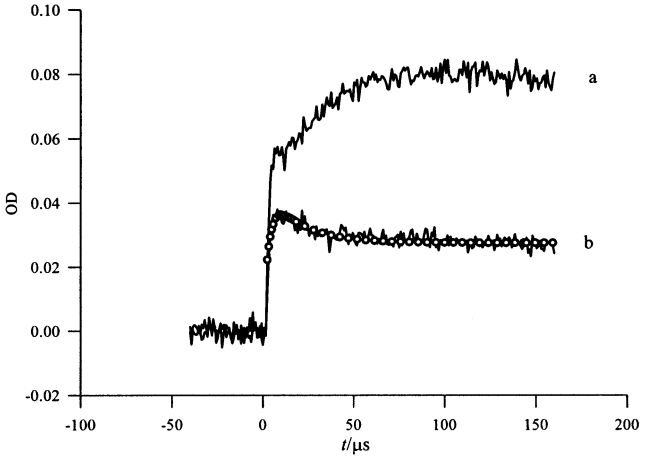

Figure 2. Traces of the transients recorded at 400 nm after a 5-Gy pulse on Ar-saturated neutral solutions of 10^{-2} M $C_6H_5N_2^+BF_4^-$: (a) without 2-propanol and (b) with 0.5 M 2-propanol. The curve (○) shows the best fit to eqs 9 and 10 with the following rate constants ensuing: $k_9 = 1.1 \times 10^7$ M^{-1} s^{-1}, $k_{-9} = 1.1 \times 10^5$ s^{-1}, and $k_{10} = 1.5 \times 10^5$ s^{-1}.

Under our conditions, the formation of the strong reductant $(CH_3)_2\dot{C}OH$ in eqs 4, 5, and 7 does not seem to initiate a chain process involving the reactions of eqs 7, 9, 10, and 14 depicted below.

$$(CH_3)_2\dot{C}OH + X-C_6H_4N_2^+ \xrightarrow{k_{14}} (CH_3)_2CO + H^+ + X-C_6H_4N_2^{\bullet} \quad (14)$$

No differences were observed in the spectra recorded after the first, second, or even tenth pulse. However, it should be mentioned that chain processes involving alcohols and diazonium salts are well-known,[33,34] and indeed their presence was also observable herein for X = F at large salt concentrations. We did not pursue this point further.

The kinetics and spectral features of $(X-C_6H_4)_2N_4^{\bullet+}$ were studied in the presence of 0.1−0.5 M 2-propanol at $\lambda \geq 380$ nm. For X = $COOC_2H_5$, F, H, and CH_3 the maxima were located at lower wavelengths, but filters with cutoff values at $\lambda = 380$ nm had to be used in order not to photolyze the rather labile diazonium salts. The spectra are collected in Figure 3.

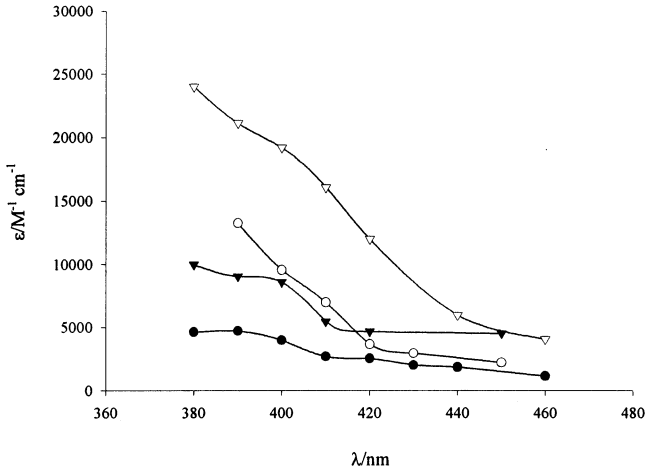

Figure 3. Absorption spectra of $(X-C_6H_4)_2N_4^{\bullet+}$ for X = $COOC_2H_5$ (●), F (○), H(▼), and CH_3(▽).

The rate constants k_9, k_{-9}, and k_{10} as well as the extinction coefficients of $(X-C_6H_4)_2N_4^{\bullet+}$ were extracted from kinetic traces recorded for 4−6 different substrate concentrations by employing the simulation program Gepasi 3.21 (see Figure 2).[31] Whereas k_9 is precisely determined by this procedure, quite a large variation can be tolerated for the values of k_{-9} and k_{10} without affecting the decay of $(X-C_6H_4)_2N_4^{\bullet+}$, which is mainly influenced by their combined effect. In principle, the values of the two rate constants could even be interchanged for such a mechanism if it stood alone. However, since the specific rates of these reactions exert a strong influence on the kinetics of the follow-up reaction between $X-C_6H_4^{\bullet}$ and $X-C_6H_4N_2^{+}$, eq 11, it was found that k_{10} had to be set equal to the larger of the two values for all substituents except $N(CH_3)_2$.

In general, the values extracted for the rate constants were found to be independent of the substrate concentration, the only exception being for X = CH_3, where the variation in k_{10} was almost 10-fold in going from 1.3×10^4 s^{-1} at a salt concentration of 3.3×10^{-4} M to 1.0×10^5 s^{-1} at 0.02 M. Also, k_{-9} showed a large variation of $(0.7-4.2) \times 10^4$ s^{-1}, whereas the values determined for k_9 were constant. In this case, the reaction mechanism might be much more complex in the sense that the lifetime of the $(X-C_6H_4)_2N_4^{\bullet+}$ species is influenced through an interaction with yet another substrate molecule. However, since the upper limits determined for the k_{-9} and k_{10} intervals were in better agreement with the results obtained for the other substituents, we selected these values in the further treatment of the data.

For the two strongest electron-donating groups, OCH_3 and $N(CH_3)_2$, the kinetics exhibited some distinct features. In the case of X = $N(CH_3)_2$, the buildup seemed to have two components at the highest concentrations employed as observed for the electron-withdrawing substituents, but the absorption maximum was shifted substantially to a wavelength of 660 nm. This indicates that the structure of the $(X-C_6H_4)_2N_4^{\bullet+}$ species is quite different in this case. Unfortunately, addition of 2-propanol did not completely remove the second component, preventing us from recording the spectrum. Rather, it resulted in an equally large decrease of both parts, suggesting either that the diazenyl and the aryl radicals in this particular case should be scavenged by exactly the same rate or that an alternative mechanism is in play, where $(X-C_6H_4)_2N_4^{\bullet+}$ is transformed directly to $(X-C_6H_4)_2N_2^{\bullet+}$ through the expulsion of dinitrogen. The latter possibility cannot be excluded rigorously, although it does not find support in the observation that the second buildup is dependent on the substrate concentration. In this case, the rate constants had to be extracted through a simulation of the full reaction scheme (see below).

For X = OCH_3, the formation of $(X-C_6H_4)_2N_4^{\bullet+}$ was detectable neither at the highest concentrations of the diazonium salt employed nor in the presence of 2-propanol. From a kinetic point of view, this should be attributed to either a small value of k_9 and/or a large value of k_{-9} since k_{10} is not particularly large, as the analysis of the kinetics of the follow-up reactions will reveal. However, it seems peculiar that the methoxy substituent is the only one that should exhibit such behavior. Therefore, another possibility is that $(X-C_6H_4)_2N_4^{\bullet+}$ indeed is formed but that it is not detected in this case because its spectrum is overlaid by the strong signals of the species generated in the follow-up reactions (see below). In that instance, there would be no straightforward access to the determination of the rate constants in question.

The average values obtained for rate constants k_9, k_{-9}, and k_{10} from the fits of the kinetic traces recorded at different substrate concentrations are gathered in Table 1 along with the calculated equilibrium constant $K = k_9/k_{-9}$. In general, the nature of the substituent does not have a great influence on the parameters. The values of k_9 are all in the range of $(0.7-1.9) \times 10^7$ M^{-1} s^{-1}, and along with the finding that $K > 100$ M^{-1}, it shows that the formation of $(X-C_6H_4)_2N_4^{\bullet+}$ is favorable for all X.

An important question in this context is related to the exact structure of $(X-C_6H_4)_2N_4^{\bullet+}$, or put differently, at which position(s) of $X-C_6H_4N_2^{+}$ does $X-C_6H_4N_2^{\bullet}$ attack? The fact that λ_{max} is much higher for X = $N(CH_3)_2$ than for X = $COOC_2H_5$, F, H, and CH_3 points to the possibility that whereas the attack in the former case takes place at the terminal nitrogen atom, thereby forming a highly conjugated tetraazadiene radical cation, the attack in the latter cases rather occurs at the π system of the phenyl ring. On energetic grounds, it seems to be precluded that the diazenyl radicals actually should break the aromaticity of the phenyl ring in an addition reaction whereas the formation of simple π-complexing adducts as suggested for the interaction of diazenyl radicals with olefins is a much more likely reaction pathway.[35,36] This would also be in line with the observation that there is essentially no substituent effects on the extracted data.

In Table 1, the fragmentation rate constants of the diazenyl radicals, k_{10} (column 6), are compared with corresponding literature values obtained by pulse radiolysis in water (column 7)[22] and EPR spectroscopy in cyclopropane (column 8).[35,36] A few thermolysis studies have also been carried out in nonpolar solvents.[37,38] These literature data and their origin deserve some comment. In a previous pulse radiolysis study on diazonium salts using high doses of up to 100 Gy, it was assumed that the main pathway consisted of the dimerization of $X-C_6H_4N_2^{\bullet}$.[22] On this basis, competition experiments involving the dimerization reaction and the first-order fragmentation of the diazenyl radicals allowed a rough estimation of the rate constant for the latter reaction. A problem associated with this procedure is the neglect of the substantial contribution from the appearance of radical cations in the absorption spectra, as revealed by our experiments. In this respect, EPR spectroscopy is a better technique, as it allows direct detection of the diazenyl radicals formed upon photolysis of the pertinent aryltriphenylmethyl azo compounds.[35,36] The disadvantage, however, is that the measurements have to be carried out at low temperature in a solvent such as cyclopropane to ensure a sufficiently large steady-state concentration of free radicals. The k_{10} values listed at 20 °C in Table 1 are therefore extrapolated by us from Arrhenius plots. Note that these extrapolated values show no clear-cut substituent

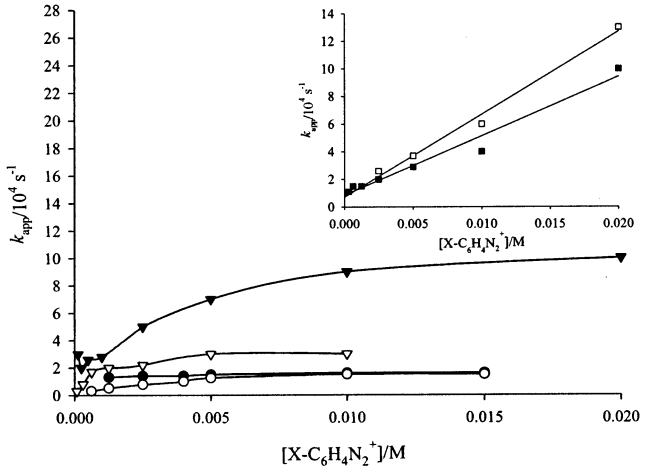

Figure 4. Apparent rate constant k_{app} of the buildup of $(X-C_6H_4)_2N_2^{\bullet+}$ as a function of the concentration of $X-C_6H_4N_2^+BF_4^-$ obtained for X = $COOC_2H_5$ at 400 nm (●), X = F at 410 nm (○), X = OCH_3 at 620 nm (▼), and X = $N(CH_3)_2$ at 660 nm (▽). Inset: equivalent plots obtained for X = H (■) and CH_3 (□) at 410 and 380 nm, respectively.

dependency, contrary to the situation at −96 °C, where a ρ value as large as +1.53 was obtained from a Hammett plot of log k_{10} versus σ.[35,36] The reason that electron-donating substituents should have a stabilizing effect on the aryldiazenyl radical is the induction of a negative polarization at the N═N group.[39]

The k_{10} values determined in this work are 1−2 orders of magnitude smaller than the values obtained in the previous pulse radiolysis study. In addition, we find no appreciable substituent effect on k_{10}. As mentioned above, we believe that the reason for these differing results should be ascribed to the kinetic interpretations. In most cases, the present values, which are in the range of $(0.4-4.0) \times 10^5\ s^{-1}$, are comparable to or slightly smaller than the extrapolated EPR data of $(1.1-1.7) \times 10^5\ s^{-1}$ in cyclopropane. Indeed, water would be expected to stabilize the quite polar diazenyl radicals better than cyclopropane. We therefore believe that the EPR data support our interpretation of the pulse radiolysis kinetics.

Kinetics of Equations 11−13. The second and slower buildup observed in the kinetic traces (see Figure 1) is attributed to the formation of $(X-C_6H_4)_2N_2^{\bullet+}$, eq 11, and eventually its further reaction with water to afford the corresponding OH adduct, $(X-C_6H_4)_2N_2OH^{\bullet}$, as shown in eq 12. Other possible decay pathways consist of second-order processes involving any of the radicals and radical cations present (eq 13). The kinetics of the buildup and the subsequent decay was studied at different diazonium salt concentrations in the range of 6.25×10^{-5} to 0.02 M. Overall, the kinetic behavior was the same, independent of the substituent, even though some distinct features also were present.

Figure 4 shows plots of the apparent pseudo-first-order rate constant, k_{app}, of the buildup of $(X-C_6H_4)_2N_2^{\bullet+}$ as a function of the diazonium salt concentration. Whereas a reasonable linear correlation is obtained in the cases of X = H and CH_3 throughout the concentration interval, an asymptote appears for X = $N(CH_3)_2$, OCH_3, F, and $COOC_2H_5$ at the highest concentrations employed. The asymptotic behavior is particularly pronounced for X = $COOC_2H_5$ with almost no variation in the rates at all. This is related to the fact that the kinetic control is mainly by the reverse reaction of eq 9 and the reaction of eq 10 with their low values of k_{-9} and k_{10} rather than by the substrate-dependent eq 11. However, too much emphasis should not be put on these roughly determined k_{app} values because of the complex nature of the reaction scheme. Both the "delay" in the formation of the aryl radicals due to the intermediacy of the $(X-C_6H_4)_2N_4^{\bullet+}$ species at large concentrations and the influence of the decays pertaining to the different radical cations and radicals shown in eqs 12 and 13 at lower concentrations are not properly accounted for.

The asymptote holds quite important information about which of the two parameters k_{-9} and k_{10} extracted from the first part of the traces is the larger one. As mentioned above, these rate constants may be interchanged without affecting the kinetics of eqs 9 and 10, but this does not hold for the kinetics of eqs 11−13. The fragmentation rate constant of the diazenyl radical, k_{10}, is the main parameter governing the formation rate of the aryl radicals, so the larger k_{10} becomes, the larger value the asymptote can attain. Note that for X = OCH_3 the asymptotic value would simply correspond to k_{10} on the assumption that the formation of $(X-C_6H_4)_2N_4^{\bullet+}$ is absent.

The determination of the rate constant for the buildup of $(X-C_6H_4)_2N_2^{\bullet+}$, k_{11}, and the apparent rate constant of its decay, denoted $k_{12/13}$, required the simulation of the complete reaction scheme using the program Gepasi 3.21.[31] For all substituents except $N(CH_3)_2$, the two buildups could be treated independently in the sense that rate constants k_9, k_{-9}, and k_{10} obtained previously were kept fixed in the program; the input values used for k_{11} were calculated from the k_{app} values extracted from Figure 4. For the dimethylamino substituent only, we found that the best and most consistent fits were obtained when $k_{-9} > k_{10}$. For X = OCH_3, k_9 was set equal to zero to account for the fact that the formation of $(X-C_6H_4)_2N_4^{\bullet+}$ did not seem to occur. However, as discussed above, the validity of this procedure is uncertain, as we cannot exclude the possibility that the spectrum of $(X-C_6H_4)_2N_4^{\bullet+}$ is simply not observable in this case because it is overlaid by that of $(X-C_6H_4)_2N_2^{\bullet+}$.

According to the reaction scheme, $k_{12/13}$ is a composite of mixed-order rate constants, and indeed dose-variation experiments revealed that the first-order decay was partly mixed with second-order processes at high doses. However, for the sake of computational simplicity, the values of $k_{12/13}$ were assumed to be first order in all simulations (and are thus given in units of s^{-1}). Finally, it should be noted that the corresponding buildup of the products formed in these reactions was detectable (but not easily discernible) at wavelengths of about 400 nm. Examples illustrating the simulation procedure are shown in Figures 5 and 6 for X = $N(CH_3)_2$ and OCH_3.

For X = $COOC_2H_5$, F, H, and CH_3, the kinetics was more complex because the spectra had contributions from species originating from the reaction between $HO^{\bullet}$ and $X-C_6H_4N_2^+$, as described elsewhere.[24] In these cases, we had to accept the uncertainties introduced by their presence, and we found that the best and most consistent procedure for determining the rate constants was from plots of the maximal OD versus the salt concentration, as shown in Figure 7. The thus-extracted rate constants, k_{11} and $k_{12/13}$, are collected in Table 1.

Because of the uncertainties involved in this procedure, we wished to substantiate our results through a determination of k_{11} on the basis of competition kinetics. A series of measurements were therefore carried out in the presence of molecular oxygen, taking advantage of its efficiency as a scavenger of aryl radicals according to eq 15.

$$X-C_6H_4^{\bullet} + O_2 \xrightarrow{k_{15}} X-C_6H_4O_2^{\bullet} \qquad (15)$$

By varying the concentration of oxygen, a competition was introduced between the reactions of eqs 11 and 15. This provided direct access to k_{11}, as k_{15} could be determined independently

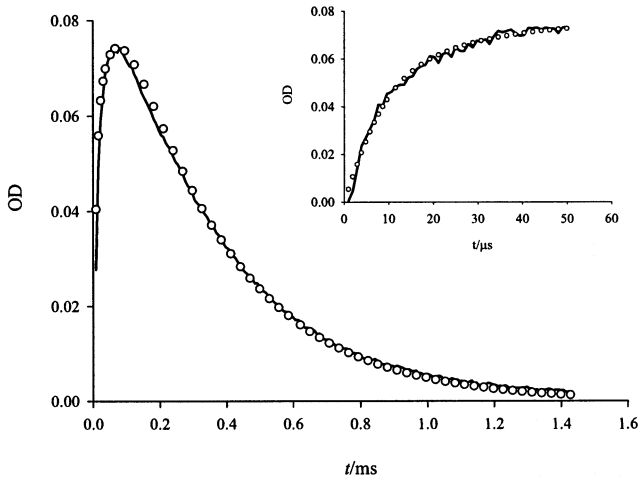

Figure 5. Trace of the transients recorded at 660 nm after a 1-Gy pulse on an Ar-saturated neutral solution of 5×10^{-3} M $(CH_3)_2N-C_6H_4N_2^+BF_4^-$. Inset: snapshot of the buildup revealing its two constituents. The open circles (○) in the two plots show the best fit to the complete reaction scheme, eqs 9−13, with the following rate constants ensuing: $k_9 = 1.2 \times 10^7$ M^{-1} s^{-1}, $k_{-9} = 7.0 \times 10^4$ s^{-1}, $k_{10} = 4.0 \times 10^4$ s^{-1}, $k_{11} = 6.6 \times 10^7$ M^{-1} s^{-1}, and $k_{12/13} = 3200$ s^{-1}. At this wavelength, an extinction coefficient of 60 000 M^{-1} cm^{-1} was used for both $(X-C_6H_4)_2N_4^{\bullet+}$ and $(X-C_6H_4)_2N_2^{\bullet+}$.

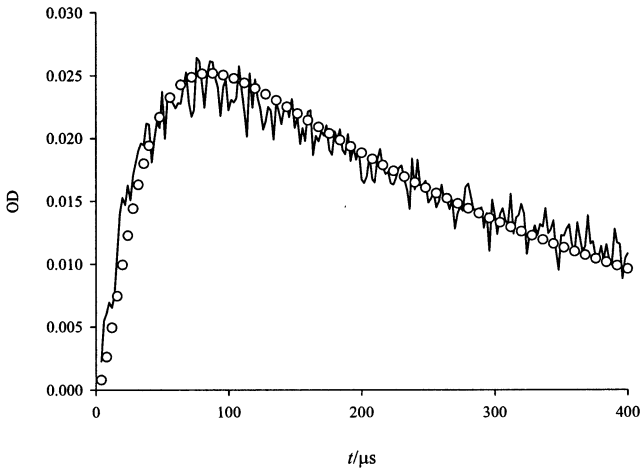

Figure 6. Trace of the transient recorded at 620 nm after a 0.83-Gy pulse on an Ar-saturated neutral solution of 10^{-3} M $CH_3O-C_6H_4N_2^+BF_4^-$. The open circles (○) show the best fit to the reaction scheme, eqs 10−13, with the following rate constants ensuing: $k_{10} = 1.0 \times 10^5$ s^{-1}, $k_{11} = 3.6 \times 10^7$ M^{-1} s^{-1}, and $k_{12/13} = 3400$ s^{-1}.

by studying the buildup of the peroxyl radicals generated upon pulse radiolysis of partially oxygenated solutions containing the corresponding substituted bromobenzenes.[40] The values of k_{15} are gathered in Table 2 along with the characteristic spectral data for the peroxyl radicals. The rate data are all found to be large ($k_{15} \approx 2 \times 10^9$ M^{-1} s^{-1}) and in reasonable agreement with literature values.[26]

The experiments were carried out at high diazonium salt concentrations of 0.1 M for X = $COOC_2H_5$, F, H, and CH_3 and 0.2 M for X = OCH_3 to ensure that the aryl radicals were completely scavenged by either the salts or oxygen and therefore not consumed in the reactions of eq 13. In the case of X = $N(CH_3)_2$, the concentration had to be lowered to 10^{-3} M to suppress a slow reaction occurring between the salt and oxygen that turned the stock solution brownish after a few minutes. As the oxygen concentration was raised, the spectrum of the radical cations was gradually replaced by that of the peroxyl radicals in accordance with the intermediacy of aryl radicals.[41] These

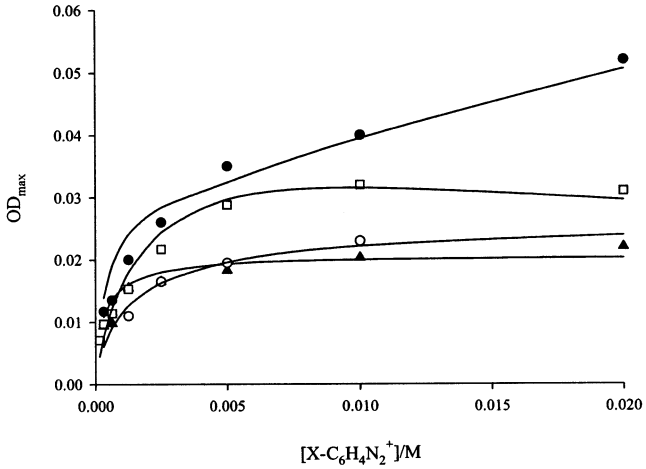

Figure 7. Maximal optical density, OD_{max}, of the transients generated after 2.5-Gy pulses on Ar-saturated neutral solutions of $X-C_6H_4N_2^+BF_4^-$ as a function of the salt concentration for X = $COOC_2H_5$ at 400 nm (□), X = F at 410 nm (○), X = H at 410 nm (▲), and X = CH_3 at 380 nm (●). The solid curves are fits based on the simulation of the whole reaction scheme, eqs 9−13, where the previously determined values of k_9, k_{-9}, and k_{10} are kept fixed (see Table 1).

TABLE 2: Spectral Features and Rate Constant, k_{15}, for the Buildup of Substituted Phenylperoxyl Radicals, $X-C_6H_4O_2^{\bullet}$

X	λ_{max} nm	ϵ_{max} M^{-1} cm^{-1}	k_{15} 10^9 M^{-1} s^{-1}
$COOC_2H_5$	475	900 ± 90	2.5 ± 0.4
F	510	1420 ± 100	2.5 ± 0.5
H	490 (490)[a]	1230 ± 80 (1300)[a]	2.6 ± 0.5 (3.3)[a]
CH_3	540 (560)[a]	1130 ± 150 (600)[a]	1.6 ± 0.3
OCH_3	600 (590)[a]	1800 ± 120 (1900)[a]	2.1 ± 0.5 (3.2)[a]
$N(CH_3)_2$	(600)[a]	(1200)[a]	2.1[b]

[a] From ref 26. [b] Assumed to be the same as for X = OCH_3; reliable results could not be obtained because the solubility of 4-bromo-*N*,*N*-dimethylaniline in water is too low.

competition data led to the determination of rate constant k_{11} through eq 16.

$$OD_{ratio} \equiv \frac{OD_{radical\ cation} - OD_{measured}}{OD_{measured} - OD_{peroxyl}} = \frac{k_{15}}{k_{11}[X-C_6H_4N_2^+]}[O_2] \quad (16)$$

The relevant plots are shown in Figure 8 with the extracted values of k_{11} collected in column 10 of Table 1.

The excellent agreement between the two data sets of k_{11} in columns 9 and 10 strongly supports our interpretation of the reaction kinetics. Interestingly, the k_{11} values pertaining to the formation of $(X-C_6H_4)_2N_2^{\bullet+}$ exhibit a rather pronounced substituent effect contrary to the k_9 values pertaining to the formation of the π-complexing adducts $(X-C_6H_4)_2N_4^{\bullet+}$. Without comparison, the fastest attack by the aryl radicals occurs on the diazonium salts having the two strongest electron-donating groups, $N(CH_3)_2$ and OCH_3, because of their stabilizing effect on the positive charge of $(X-C_6H_4)_2N_2^{\bullet+}$.

Identification of Intermediates. Structural information about the species produced in the reaction between $X-C_6H_4^{\bullet}$ and $X-C_6H_4N_2^+$ can be obtained from the spectra collected in Figure 9. Although the risk of photolysis of the parent diazonium salts prevented us from recording spectra below 380 nm, there is no doubt that the maxima are located in this region for X =

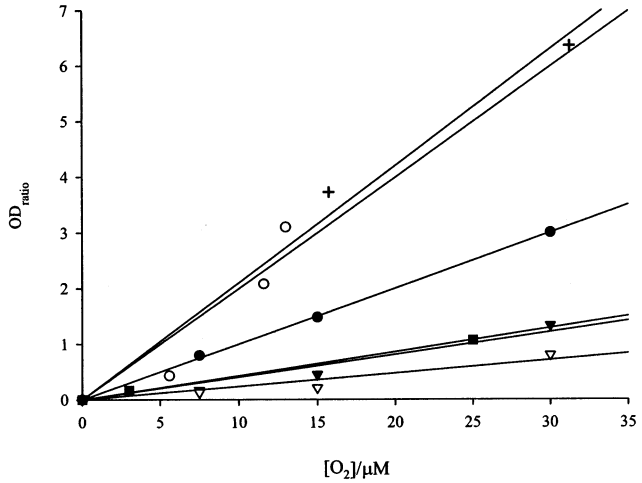

Figure 8. Plot of the parameter OD_{ratio} as a function of the concentration of oxygen for X = $COOC_2H_5$ at 400 nm (●), X = F at 410 nm (○), X = H at 380 nm (▼), X = CH_3 at 380 nm (▽), X = OCH_3 at 600 nm (+), and X = $N(CH_3)_2$ at 660 nm (■). In the case of X = OCH_3, the oxygen concentration has been divided by a factor of 40 to encompass the plot in the Figure. The concentration of the diazonium salts was 0.1 M for all substituents except $N(CH_3)_2$ and OCH_3 in the cases in which 10^{-3} and 0.2 M were employed, respectively.

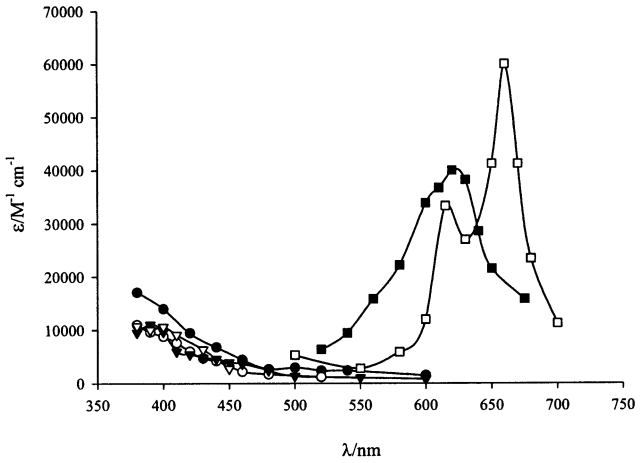

Figure 9. Absorption spectra of $(X-C_6H_4)_2N_2^{\bullet+}$ for X = OCH_3 (■) and X = $N(CH_3)_2$ (□) and absorption spectra of $(X-C_6H_4)_2N_2OH^{\bullet}$ for X = $COOC_2H_5$ (●), X = F (○), X = H (▼), and X = CH_3(▽) recorded in Ar-saturated neutral solutions. The extinction coefficients were obtained from the best fits of the kinetics. Note that the spectra in the last four cases also may include other species derived from the OH adducts of the diazonium salts.

$COOC_2H_5$, F, H, and CH_3. For X = OCH_3 and $N(CH_3)_2$, however, distinct absorption maxima appear at 620 and 660 nm, respectively. Clearly, such differences in the absorption spectra must be attributed to large structural differences of the intermediates produced. One working hypothesis would be that $(X-C_6H_4)_2N_2^{\bullet+}$ for X = OCH_3 and $N(CH_3)_2$ simply corresponds to the radical cations of the corresponding azobenzenes (i.e., the aryl radicals have attacked the terminal nitrogen on the diazonium salts). For the remaining substituents, the radical cations are less stable, and they are immediately transformed to the corresponding OH adducts, eq 12, as illustrated in Scheme 2.[42]

The assignment of the intermediate to the radical cation for X = OCH_3 and $N(CH_3)_2$ is supported by the observation that it was unaffected by the presence of micromolar concentrations of oxygen. Unfortunately, the concentration of oxygen could not be raised further if scavenging of the aryl radicals to arylperoxyl radicals was to be avoided. Other kinds of verification were therefore required.

A characteristic feature of radical cations is their fast reactions with reductants and bases. For instance, the rate constants for the reactions of Fe^{2+} and OH^- with the radical cation of anisole are as large as 6×10^8 and 1×10^9 M^{-1} s^{-1}, respectively.[43] For most of our systems, such processes could not be studied since the diazonium salts themselves would react with the reductant/base upon mixing.[20] However, for the two strongly electron-donating groups, OCH_3 and $N(CH_3)_2$, it was possible to carry out the study employing a stopped-flow system where Ar-saturated solutions of salt in one syringe and reductant/base in another syringe were mixed in the cell a few seconds before the electron pulse. The typical concentrations used were $[X-C_6H_4N_2^+] = 10^{-2}$ M, $[K_4Fe(CN)_6] = 10^{-6}$ to 10^{-5} M, and [NaOH] = 10^{-3} to 10^{-2} M. The pseudo-first-order decay of the radical cations was followed at a wavelength of 620 nm for X = OCH_3 and 660 nm for X = $N(CH_3)_2$. For X = OCH_3, the following values were obtained: $k(Fe^{2+}) = 7.2 \times 10^9$ M^{-1} s^{-1} and $k(OH^-) = 7.5 \times 10^6$ M^{-1} s^{-1}. For X = $N(CH_3)_2$, $k(Fe^{2+}) = 5 \times 10^9$ M^{-1} s^{-1}, whereas the experiments with base could not be carried out because the reaction between OH^- and the diazonium salt was too fast. Clearly, the finding of such large rate constants is consistent with the presence of radical cations.

Another strong piece of evidence in favor of the above interpretation would be provided if the spectra of the radical cations of the azo compounds could be obtained using alternative pathways. Actually, in pulse radiolysis, the parent azobenzenes may be oxidized quite easily using a species such as Tl^{2+} (generated from $Tl^+ + HO^{\bullet}$) in neutral solution or simply through the formation of the OH adducts of the azobenzenes followed by the elimination of water in a strongly acidic solution, as illustrated in eq 17.[43-48]

$$X-C_6H_4N{=}NC_6H_4-XOH^{\bullet} + H^+ \rightleftharpoons X-C_6H_4N{=}NC_6H_4-X^{\bullet+} + H_2O \quad (17)$$

Note that the equilibrium reaction of eq 17 is the same as that given in eq 12 and Scheme 2. In these procedures, the

SCHEME 2

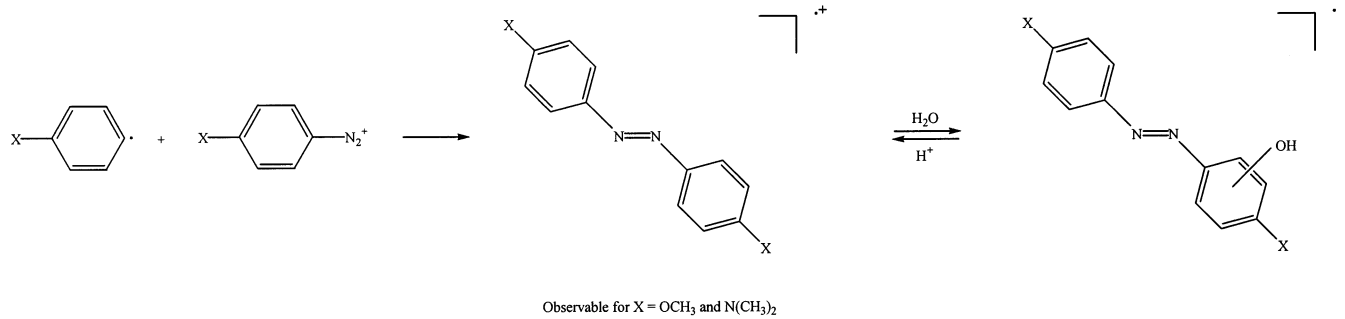

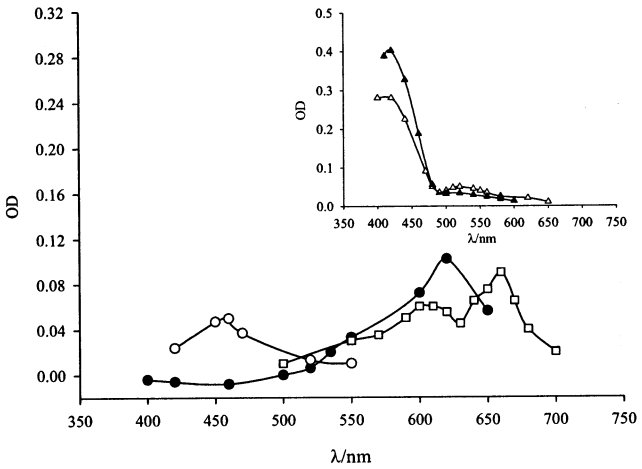

Figure 10. Absorption spectrum of the radical cation of (*E*)-4,4′-dimethoxyazobenzene generated from the parent compound after a 40-Gy pulse on an air-saturated pH 0 solution (●). Absorption spectrum of the OH adduct of (*E*)-4,4′-dimethoxyazobenzene generated from the parent compound after a 40-Gy pulse on a N_2O-saturated neutral solution (○). Absorption spectrum of the radical cation of (*E*)-4,4′-bis(dimethylamino)azobenzene generated from the parent compound after a 5-Gy pulse on a N_2O-saturated neutral solution containing 2.5×10^{-4} M Tl_2SO_4 (□). The signals in the latter spectrum have been multiplied by a factor of 10. Inset: absorption spectra of the OH adduct of (*E*)-azobenzene generated from the parent compound after 40- and 3.3-Gy pulses, respectively, on N_2O-saturated neutral solutions without (▲) and with (△) 2.5×10^{-4} M Tl_2SO_4. The signals in the latter spectrum have been multiplied by a factor of 5.

extremely low solubility of the azo compounds in aqueous solution presented a major problem, but in most experiments, it could be increased sufficiently for the recording of qualitative spectra by employing a combination of heating and ultrasound[49] or preferentially extensive stirring. Because of incomplete scavenging, the extinction coefficients could not be calculated in these cases.

In Figure 10, the spectra pertaining to the oxidation products of (*E*)-4,4′-dimethoxyazobenzene, (*E*)-4,4′-bis(dimethylamino)-azobenzene, and (*E*)-azobenzene are shown. In the case of (*E*)-4,4′-dimethoxyazobenzene, the same species could be generated in neutral solution using Tl^{2+} as an oxidant (not shown) and in strongly acidic solution from the OH adduct; the negative OD values below $\lambda = 500$ nm are due to the self-absorption of (*E*)-4,4′-dimethoxyazobenzene. This species with the very same absorption peak at 620 nm as observed upon the pulse radiolytic reduction of $CH_3O-C_6H_4N_2^+$ (see Figure 9) showed no reactivity toward oxygen, and it is therefore assigned to the pertinent radical cation.[50] Moreover, in a N_2O-saturated neutral solution, where e_{aq}^- is converted to $HO^•$, it was possible to detect both species in the equilibrium reaction of eq 17 (i.e., the radical cation as well as the OH adduct of (*E*)-4,4′-dimethoxyazobenzene). The spectrum of the OH adduct with a charateristic peak at 460 nm is also included in Figure 10. The observation that the maximum for the radical cation appears at a substantially longer wavelength than for the corresponding OH adduct is also known from studies on biphenyl[45] and naphthalene.[48]

The corresponding results obtained for (*E*)-4,4′-dimethylaminoazobenzene are completely in line with the above interpretation as illustrated in Figure 10. In neutral solution, the oxidation of the azo compound by Tl^{2+} gives rise to an absorption spectrum with the characteristic peaks at 610 and 660 nm, as observed in the pulse radiolysis experiments on $(CH_3)_2N-C_6H_4N_2^+$ (see Figure 9). When the pH is lowered, an interesting development takes place in the sense that the peak observed at 660 nm vanishes (not shown). This phenomenon is due to the protonation of one of the dimethylamino groups so that the species studied at low pH is a protonated radical cation. These results will be described elsewhere.[24]

The behavior of (*E*)-azobenzene differs somewhat from that of the other two azobenzenes, as there is essentially no difference between the spectra obtained when Tl^{2+} is used as an oxidant and when the OH adduct is formed in a N_2O-saturated neutral solution. As shown in the inset of Figure 10, the maximum seems to appear at about 400 nm, in line with the characteristics of the spectrum recorded upon the pulse radiolytic reduction of $C_6H_5N_2^+$ (see Figure 9). In the literature, it has been reported that the radical cation with a distinct peak at 540 nm can be generated using steady-state radiolysis of (*Z*)-azobenzene in matrixes at low temperature.[51] Thus, the species formed under our conditions is presumably the OH adduct of azobenzene, independent of pH (i.e., the equilibrium reaction of eq 17 is shifted completely toward the left). It is in accordance with expectations that the radical cation of azobenzene should be less stable than the radical cations of 4,4′-dimethoxyazobenzene and 4,4′-bis(dimethylamino)azobenzene because of the absence of the stabilizing electron-donating groups.

On the basis of the spectral information obtained, we conclude that the working hypothesis outlined in Scheme 2 is correct. For $X = OCH_3$ and $N(CH_3)_2$, the reaction between $X-C_6H_4^•$ and $X-C_6H_4N_2^+$, eq 11, leads to the formation of the radical cations of the corresponding azobenzenes before the follow-up reaction with water will produce the pertinent OH adducts. From a kinetic point of view, the measured decay rate constant $k_{12/13}$ therefore pertains to both eqs 12 and 13. For $X = COOC_2H_5$, F, H, and CH_3, the reaction scheme is still valid, but in these cases, the radical cations are attacked so quickly by water that they are not even detectable in pulse radiolysis. As a result, the decay pathway in these cases mainly pertains to eq 13. Finally, it should be noted that product analyses of steady-state radiolysis experiments are consistent with the view that the main attack by the aryl radical occurs at the diazo group rather than at the aromatic ring of the diazonium salt. Such experiments also reveal that additional reactions may take place when the time scale is larger than that of the pulse radiolysis measurements.[24]

Acknowledgment. We are indebted to Hanne Corfitzen and Torben Johansen for skilful technical assistance. We also acknowledge *Statens Naturvidenskabelige Forskningsråd* for financial support.

References and Notes

(1) Wulfman, D. S. In *The Chemistry of Diazonium and Diazo Groups*; Patai, S., Ed.; Wiley: Chichester, U.K., 1978.

(2) Zollinger, H. *Diazo Chemistry I: Aromatic and Heteroaromatic Compounds;* VCH: Weinheim, Germany, 1994.

(3) Zollinger, H. In *The Chemistry of Triple Bonded Functional Groups*; Patai, S., Rappoport, Z., Eds.; Wiley: Chichester, U.K., 1983.

(4) Galli, C. *Chem. Rev.* **1988**, *88*, 765.

(5) Barbero, M.; Degani, I.; Dughera, S.; Fochi, R. *J. Org. Chem.* **1999**, *64*, 3448.

(6) Bravo-Díaz, C.; Romsted, L. S.; Harbowy, M.; Romero-Nieto, M. E.; Gonzalez-Romero, E. *J. Phys. Org. Chem.* **1999**, *12*, 130.

(7) Steenken, S.; Ashokkumar, M.; Maruthamuthu, P.; McClelland, R. A. *J. Am. Chem. Soc.* **1998**, *120*, 11925.

(8) Cuccovia, I. M.; da Silva, M. A.; Ferraz, H. M. C.; Pliego, J. R., Jr.; Riveros, J. M.; Chaimovich, H. *J. Chem. Soc., Perkin Trans. 2* **2000**, 1896.

(9) Canning, P. S. J.; McCrudden, K.; Maskill, H.; Sexton, B. *J. Chem. Soc., Perkin Trans. 2* **1999**, 2735.

(10) Romero-Nieto, M. E.; Malvido-Hermelo, B.; Bravo-Díaz, C.; González-Romero, E. *Int. J. Chem. Kinet.* **2000**, *32*, 419.

(11) Kosynkin, D.; Bockman, T. M.; Kochi, J. K. *J. Am. Chem. Soc.* **1997**, *119*, 4846.

(12) Quintero, B.; Morales, J. J.; Quiros, M.; Martinéz-Puentedura, M. I.; del Carmen Cabeza, M. *Free Radical Biol. Med.* **2000**, *29*, 464.
(13) Geahigan, K. B.; Taintor, R. J.; George, B. M.; Meagher, D. A.; Nalli, T. W. *J. Org. Chem.* **1998**, *63*, 6141.
(14) Hanson, P.; Rowell, S. C.; Taylor, A. B.; Walton, P. H.; Timms, A. W. *J. Chem. Soc., Perkin Trans. 2* **2002**, 1126.
(15) Elofson, R. M.; Gadallah, F. F. *J. Org. Chem.* **1969**, *34*, 854.
(16) Galli, C. *J. Chem. Soc., Perkin Trans. 2* **1981**, 1459.
(17) Daasbjerg, K.; Lund, H. *Acta Chem. Scand.* **1992**, *46*, 157.
(18) Gilbert, B. C.; Hanson, P.; Jones, J. R.; Whitwood, A. C.; Timms, A. W. *J. Chem. Soc., Perkin Trans. 2* **1992**, 629.
(19) Ashworth, B.; Gilbert, B. C.; Norman, R. O. C. *J. Chem. Res., Synop.* **1977**, 94.
(20) Doyle, M. P.; Guy, J. K.; Brown, K. C.; Mahapatro, S. N.; VanZyl, C. M.; Pladziewicz, J. R. *J. Am. Chem. Soc.* **1987**, *109*, 1536.
(21) Spinks, J. W. T.; Woods, R. J. *Introduction to Radiation Chemistry*, 3rd ed.; Wiley: New York, 1990.
(22) Brede, O.; Mehnert, R.; Naumann, W.; Becker, H. G. O. *Ber. Bunsen-Ges. Phys. Chem.* **1980**, *84*, 666.
(23) Packer, J. E.; Mönig, J.; Dobson, B. C. *Aust. J. Chem.* **1981**, *34*, 1433.
(24) Daasbjerg, K.; Sehested, K. To be submitted for publication.
(25) Buxton, G. V.; Greenstock, C. L.; Helman, W. P.; Ross, A. B. *J. Phys. Chem. Ref. Data* **1988**, *17*, 513.
(26) Fang, X.; Mertens, R.; von Sonntag, C. *J. Chem. Soc., Perkin Trans. 2* **1995**, 1033.
(27) Starkey, E. B. In Organic Syntheses; Wiley & Sons: New York, 1943; Collect. Vol. 2, p 225.
(28) Yamamoto, S.; Nishimura, N.; Hasegawa, S. *Bull. Chem. Soc. Jpn.* **1971**, *44*, 2018.
(29) Vorländer, D.; Wolferts, E. *Chem. Ber.* **1923**, *56*, 1229.
(30) Sehested, K.; Corfitzen, H.; Christensen, H. C.; Hart, E. J. *J. Phys. Chem.* **1975**, *79*, 310.
(31) *Gepasi*, version 3.21; © Pedro Mendes, 1996−1999. The program may be downloaded from the Internet.
(32) Suehiro, T.; Suzuki, A.; Tsuchida, Y.; Yamazaki, J. *Bull. Chem. Soc. Jpn.* **1977**, *50*, 3324.
(33) Heighway, C. J.; Packer, J. E.; Richardson, R. K. *Tetrahedron Lett.* **1974**, 4441.
(34) Packer, J. E.; Richardson, R. K. *J. Chem. Soc., Perkin Trans. 2* **1975**, 751.
(35) Suehiro, T.; Masuda, S.; Nakausa, R.; Taguchi, M.; Mori, A.; Koike, A; Date, M. *Bull. Chem. Soc. Jpn.* **1987**, *60*, 3321.
(36) Suehiro, T. *Rev. Chem. Intermed.* **1988**, *10*, 101.
(37) Engel, P. S.; Gerth, D. B. *J. Am. Chem. Soc.* **1983**, *105*, 6849.
(38) Early CIDNP experiments (Kasukhin, L. F.; Ponomarchuk, M. P.; Buchachenkov, A. L. *Chem. Phys.* **1974**, *3*, 136) have provided a value of 10^7 s^{-1} for the fragmentation of the phenyldiazenyl radical, which appears to be an overestimation when compared with the more recent data obtained.[34−36] In this context, it should be noted that studies on alkyldiazenyl radicals have given a rate constant of about 8×10^7 s^{-1} (see: Adams, J. S.; Burton, K. A.; Andrews, B. K.; Weisman, R. B.; Engel, P. S. *J. Am. Chem. Soc.* **1986**, *108*, 7935). It would be expected that the fragmentation reaction should be faster for aliphatic than aromatic systems.
(39) INDO calculations led to a value of 2.8 D for the phenyldiazenyl radical, which is similar to the value of 2.76 D found for benzaldehyde.[36]
(40) The mechanism is described by the following reactions: $X-C_6H_4Br + e_{aq}^- \xrightarrow{-Br^-} X-C_6H_4^\bullet \xrightarrow{O_2} X-C_6H_4O_2^\bullet$. The free radicals formed upon the addition of $HO^\bullet$ to $X-C_6H_4Br$ may react with oxygen as well, but with a reaction rate that is about 10 times smaller, this will not affect the determination of k_{15}.
(41) Other evidence for the presence of aryl radicals was provided by the addition of *tert*-butanol or fumaric acid to the solution, which prevented the formation of the radical cation because of an effective scavenging of the phenyl radicals either through eq 6 or by addition to the double bond of fumaric acid.
(42) As pointed out by one of the reviewers, the addition of water might as well take place at one of the central nitrogen atoms.
(43) Holcman, J.; Sehested, K. *J. Phys. Chem.* **1976**, *80*, 1642.
(44) Sehested, K.; Holcman, J.; Hart, E. J. *J. Phys. Chem.* **1977**, *81*, 1363.
(45) Sehested, K.; Hart, E. J. *J. Phys. Chem.* **1975**, *79*, 1639.
(46) O'Neill, P.; Steenken, S.; Schulte-Frohlinde, D. *J. Phys. Chem.* **1975**, *79*, 2773.
(47) Holcman, J.; Sehested, K. *J. Phys. Chem.* **1977**, *81*, 1963.
(48) Zevos, N.; Sehested, K. *J. Phys. Chem.* **1978**, *82*, 138.
(49) von Sonntag, C.; Mark, G.; Tauber, A.; Schuchmann, H.-P. *Adv. Sonochem.* **1999**, *5*, 109.
(50) In the air-saturated solution, there is no contribution from the H adduct of the azobenzene, as the hydrogen atom will react with the oxygen present to form unreactive $HOO^\bullet$.
(51) Shida, T. *Electronic Absorption Spectra of Radical Ions*; Elsevier: Amsterdam, 1988.